Antithrombogenic property of bone marrow mesenchymal stem cells in nanofibrous vascular grafts

Craig K. Hashi[†], Yiqian Zhu[‡], Guo-Yuan Yang[‡], William L. Young[‡], Benjamin S. Hsiao[§], Karin Wang[§], Benjamin Chu[§], and Song Li[†¶]

[†]Department of Bioengineering and Center for Tissue Bioengineering, University of California, Berkeley, CA 94720; [‡]Center for Cerebrovascular Research, Departments of Anesthesia and Perioperative Care and Neurological Surgery, University of California, San Francisco, CA 94143; and [§]Department of Chemistry, Stony Brook University, Stony Brook, NY 11794

Communicated by Gabor A. Somorjai, University of California, Berkeley, CA, May 18, 2007 (received for review October 31, 2006)

Nanostructured biomaterials have tremendous potential for tissue engineering. However, the performance and integration of the nanomaterials *in vivo* are not well understood. A challenge in vascular tissue engineering is to develop optimal scaffolds and establish expandable cell sources for the construction of tissue-engineered vascular grafts that are nonthrombogenic and have long-term patency. Here, we used tissue-engineered vascular grafts as a model to demonstrate the potential of combining nanofibrous scaffolds and bone marrow mesenchymal stem cells (MSCs) for vascular tissue engineering. Biodegradable nanofibrous scaffolds with aligned nanofibers were used to mimic native collagen fibrils to guide cell organization in vascular grafts. The results from artery bypass experiments showed that nanofibrous scaffolds allowed efficient infiltration of vascular cells and matrix remodeling. Acellular grafts (without MSCs) resulted in significant intimal thickening, whereas cellular grafts (with MSCs) had excellent long-term patency and exhibited well organized layers of endothelial cells (ECs) and smooth muscle cells (SMCs), as in native arteries. Short-term experiments showed that nanofibrous scaffolds alone induced platelet adhesion and thrombus formation, which was suppressed by MSC seeding. In addition, MSCs, as ECs, resisted platelet adhesion *in vitro*, which depended on cell-surface heparan sulfate proteoglycans. These data, together with the observation on the short-term engraftment of MSCs, suggest that the long-term patency of cellular grafts may be attributed to the antithrombogenic property of MSCs. These results demonstrate several favorable characteristics of nanofibrous scaffolds, the excellent patency of small-diameter nanofibrous vascular grafts, and the unique antithrombogenic property of MSCs.

blood vessel | nanofibrous scaffold | tissue engineering | vascular remodeling

Nanostructured materials have tremendous potential for tissue engineering. Electrospinning technology can be used to generate nanofibrous scaffolds made of synthetic polymers or native matrix molecules. Electrospinning is based on the principle that the surface tension associated with a single droplet can be overcome with an applied electric field, thereby creating a Taylor cone and drawing the droplet into a stream in the direction of the field (1, 2). In the past few years, there has been a significant growth of research activities to explore the applications of electrospun nanofibers. The use of electrospinning to generate functional nanofibrous scaffolds for tissue regeneration is particularly exciting because the structure and morphology of electrospun scaffolds can be manipulated to resemble those of the extracellular matrix (ECM), therefore creating a more "familiar" environment for the cells. Synthetic polymer scaffolds, such as those composed of lactic or glycolic acids, are biocompatible, have configurable mechanical properties, and can be easily modified to incorporate proteins and peptides. Recent studies have shown that electrospun nanofibers of polymers and matrix proteins allow the adhesion, proliferation, and organized assembly of cells *in vitro* (3–8). However, the performance of nanofibrous scaffolds *in vivo* is not well understood. Here, we used a nanofibrous vascular graft as a model to investigate the remodeling of nanofibrous scaffold *in vivo*.

Cardiovascular disease is the leading cause of death in the United States. Treatment of vascular disease is accordingly a large proportion of health care expenditures. For example, every year >500,000 coronary artery bypass procedures are performed. However, the use of arterial and venous grafts necessitates surgical harvest and the associated morbidity and cost. Currently available synthetic vascular grafts are limited to large internal diameter (>5 mm) grafts because of frequent thrombosis and occlusion. To overcome these limitations, we explored a tissue engineering approach to construct small-diameter vascular grafts.

Native blood vessels have three distinct layers: a potently antithrombogenic endothelial cell (EC) monolayer, a medial layer that is mainly populated by aligned smooth muscle cells (SMCs) embedded in three-dimensional ECM (mainly collagens and elastin), and an adventitial layer of connective tissue. In the past, SMCs and ECs, in combination with ECM or polymers, have been used to fabricate tissue-engineered vascular grafts (TEVGs) (9–13). Although significant progress has been made, reliable and expandable cell sources, especially nonimmunogenic cell sources, for the construction of vascular grafts have not been established and scaffolds need to be optimized.

Bone marrow is one of the most abundant sources for adult stem cells. Bone marrow MSCs can differentiate into a variety of cell types (14, 15), can be expanded millions of folds in culture, and can modulate immune responses by suppressing both B and T cell functions (16, 17). Thus, it may be feasible to use bone marrow MSCs to construct autologous or allogeneic (off-the-shelf) TEVGs. However, whether MSCs have an antithrombogenic property or whether other cells (e.g., ECs) are needed to prevent thrombosis remains unexplored.

In this study, we used TEVGs as a model to demonstrate the potential of combining nanofibrous scaffolds and bone marrow

Author contributions: C.K.H. and Y.Z. contributed equally to this work; C.K.H., Y.Z., G.-Y.Y., W.L.Y., and S.L. designed research; C.K.H., Y.Z., and K.W. performed research; G.-Y.Y., W.L.Y., B.S.H., and B.C. contributed new reagents/analytic tools; C.K.H. and Y.Z. analyzed data; and C.K.H., Y.Z., and S.L. wrote the paper.

The authors declare no conflict of interest.

Abbreviations: CCA, common carotid artery; EC, endothelial cell; ECM, extracellular matrix; MHC, myosin heavy chain; MSC, mesenchymal stem cell; PLLA, poly(L-lactic acid); SMC, smooth muscle cell; TEVG, tissue-engineered vascular graft.

[¶]To whom correspondence should be addressed at: Department of Bioengineering, University of California, 471 Evans Hall, Berkeley, CA 94720-1762. E-mail: song_li@berkeley.edu.

This article contains supporting information online at www.pnas.org/cgi/content/full/0704581104/DC1.

MSCs for vascular tissue engineering. We showed that nanofibrous TEVGs facilitated efficient cell recruitment and organization, significant ECM synthesis and self-assembly, and excellent long-term patency. Furthermore, we revealed the antithrombogenic properties of MSCs and the underlying mechanism, which may have significant impact on the use of MSCs for vascular tissue engineering and regenerative medicine.

Results

Fabrication and Characterization of Nanofibrous Scaffolds. For scaffolds, it is desirable to use materials that are biocompatible, biodegradable (in tune with tissue remodeling), bioactive, mechanically durable, and similar to the ECM structure in native blood vessels. We used electrospinning technology to fabricate nanofibrous scaffolds from poly(L-lactic acid) (PLLA), an FDA-approved, biodegradable, and biocompatible polymer. The cells and ECM fibrils in the vascular wall aligned in the circumferential direction (Fig. 1*a*). To simulate the dimension and microstructure of native collagen fibrils in the wall of a native artery, we applied uniaxial stretch to electrospun PLLA membranes and produced PLLA membranes with aligned electrospun nanofibers ≈0.5–1 μm in diameter (Fig. 1*b*). The membranes were ≈50 μm thick and highly porous, which allowed the homing and penetration of cells into the membranes for tissue regeneration. These membranes were mechanically durable with a Young's modulus of 12 MPa, which was similar to that of the native vessel.

To determine the interactions of SMCs and MSCs with nanofibrous membranes, *in vitro* experiments were performed by seeding human SMCs and MSCs on nanofibrous membranes. SMCs and MSCs seeded on membranes with aligned nanofibers (Fig. 1 *c* and *d*) had cellular organization and alignment similar to that of the native artery, suggesting that nanofibrous scaffolds mimicked native collagen fibrils and guided cell organization.

Fabrication of TEVGs. To construct a vascular graft, MSCs were seeded on a nanofibrous membrane (Fig. 1*e*) and rolled around a 0.7-mm mandrel (Fig. 1*f*). The mandrel was removed, yielding a tubular shape with MSCs embedded within the walls of the graft. Three days later, the graft was implanted into the common carotid artery (CCA) by using a bypass procedure (Fig. 1*g*).

Live/dead assays were performed to determine whether cells survived after the rolling process and surgical procedures. After a 1-d incubation period after physical handling (rolling and removal from the mandrel), almost all of the cells were calcein-positive (live) and ethidium bromide-negative (dead) (data not shown). This finding suggested that the cells were not detrimentally affected by the physical handling and were viable at the preimplantation period. Another live/dead assay was performed on a graft adjacent to an MSC graft that was being implanted to determine the viability of the cells during the suturing procedure. The graft was immersed in the interstitial cavity fluids and Dulbecco's modified Eagle's medium (DMEM) was dripped onto the graft during the surgery. Almost all of the cells were calcein-positive and ethidium bromide-negative after surgery, indicating that they were viable at all stages during implantation (Fig. 1*h*).

Cell Organization in TEVGs. We implanted the grafts into rats for up to 60 d and examined the remodeling of vascular grafts *in vivo*. After 60 d, acellular grafts had significant intimal thickening and inward remodeling in the lumen (Fig. 2*a*), suggesting that nanofibrous scaffold alone could not remain patent in the long term. In contrast, MSC-seeded vascular grafts showed little intimal thickening, suggesting that MSCs could block the inflammatory responses induced by nanofibrous scaffolds (Fig. 2*b*).

To determine the cellular components and organization in the vascular grafts, cross-sections of the vascular grafts were stained for CD31 and myosin heavy chain (MHC) to locate EC and SMC, respectively. CD31 staining showed that the lumen of both acellular and cellular grafts was covered with an EC monolayer (Fig. 2 *c* and *d*), suggesting that ECs from the host contribute to the endothelialization process in the vascular grafts. Temporal analysis demonstrated that the lumen surface of the grafts were negative for ECs after 7 d, and the endothelialization of vascular grafts could be achieved within 1 month in both acellular and cellular grafts (data not shown). Interestingly, some ECs were identified in the outer layer of the grafts or within the vascular wall (Fig. 2 *c* and *d*), suggesting that there might be angiogenesis within the grafts. Indeed, when we retrieved vascular grafts from animals, the invasion of some microvessels into the grafts from the surrounding tissue was visible.

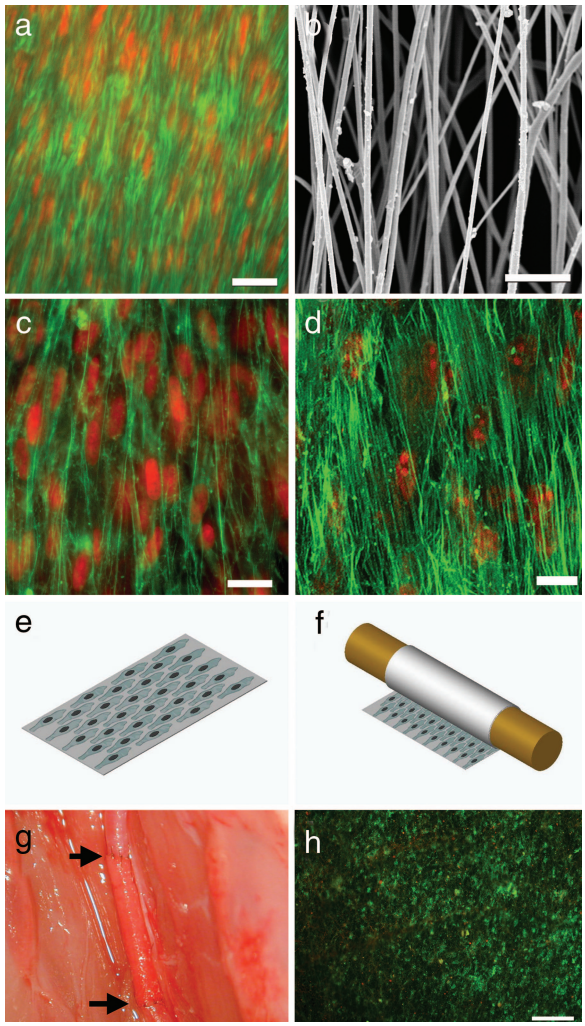

Fig. 1. Characterization of biomimetic cell–scaffold interactions. (*a*) *En face* staining of SMCs in a native rat CCA after EC denudation. The samples were stained for actin filaments by using FITC-conjugated phalloidin (green), and they were counterstained for nuclei by using propidium iodide (red). (Scale bar, 20 μm.) (*b*) SEM of aligned nanofibers made from PLLA. (Scale bar, 10 μm.) (*c*) Human aortic SMCs seeded on aligned nanofiber surface, with same staining as in *a*. (Scale bar, 20 μm.) (*d*) MSCs seeded on aligned nanofiber surface, with same staining as in *a*. (Scale bar, 20 μm.) (*e*) Schematic illustration of cells seeded on a piece of nanofibrous membrane coated with fibronectin. (*f*) Embedding cells in the tubular grafts by rolling the nanofibrous membrane. (*g*) An end-to-end anastomosis procedure of the vascular graft sutured to the CCA in a rat. The arrows indicate the two ends of the graft. (*h*) Cell survival in a vascular graft after surgery process. *En face* live/dead staining of a TEVG was performed to show calcein-positive (live) cells in green and ethidium bromide-positive (dead) cells in red. (Scale bar, 200 μm.)

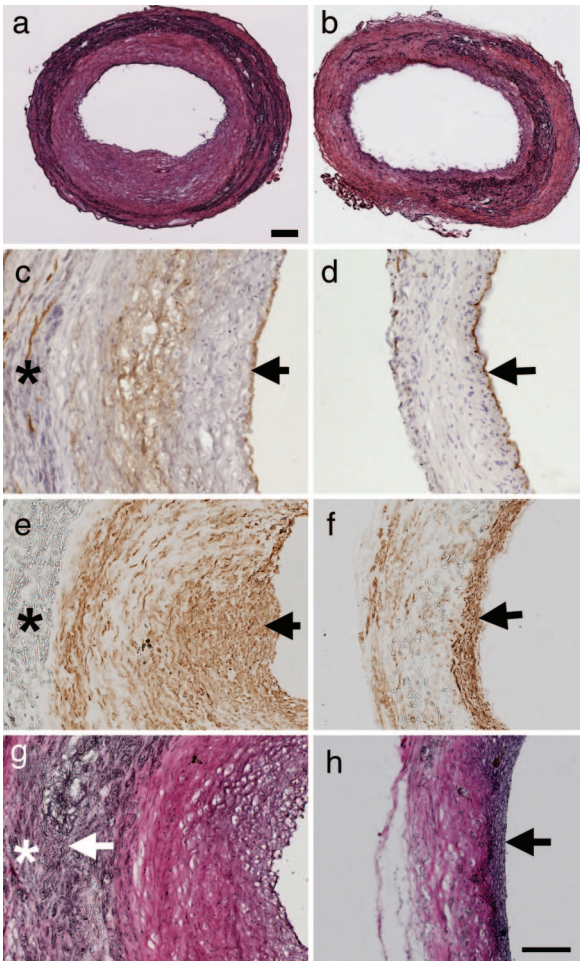

Fig. 2. Cell organization and ECM remodeling after 60 d for acellular and cellular small-diameter nanofibrous vascular grafts. Images are representatives from at least three independent samples. (*a* and *b*) Hematoxylin/eosin (H&E) staining of a cross-section in an acellular graft (*a*) and a cellular (MSC-seeded) graft (*b*) 60 d after implantation. (Scale bar, 100 μm.) (*c* and *d*) CD31 staining of cross-sections for ECs in acellular (*c*) and cellular (*d*) vascular grafts. The samples were counterstained with H&E. CD31 staining is shown in brown. Arrows indicate EC monolayer on the lumen surfaces. (*e* and *f*) MHC staining of cross-sections for SMCs in acellular (e) and cellular (*f*) vascular grafts. MHC staining is shown in brown. Arrows indicate SMCs. (*g* and *h*) ECM remodeling in acellular (*g*) and cellular (*h*) vascular grafts. Verhoeff's elastic staining of cross-sections highlights collagen (pink) and elastin (black). Arrows indicate positive elastin staining. (Scale bar: *c*–*h*, 100 μm.) *, area with PLLA polymer.

Both early (α-actin; data not shown) and late (MHC) markers were used to confirm the presence of SMCs. The acellular grafts at both 30 (data not shown) and 60 d stained positively for SMC markers (Fig. 2*e*). SMCs were widely distributed within the graft wall, with most of the SMCs in the area with intimal thickening. All MSC-seeded grafts at 60 d showed SMC-positive staining in a tight, confined band adjacent to the lumen (Fig. 2*f*) and did not show significant intimal hyperplasia. The well organized EC and SMC distribution in MSC-seeded grafts simulated that in native arteries, suggesting that cellular nanofibrous scaffolds allowed self-assembly and remodeling of vascular grafts *in vivo* and that long-term patency of cellular grafts could be achieved.

ECM Remodeling in TEVGs. ECM remodeling is another critical factor for the long-term stability of vascular grafts. To determine the synthesis and remodeling of ECM in the wall of vascular grafts, cross-sections of MSC-seeded vascular grafts were stained for collagen and elastin, the main structural ECM components in a native artery. At 1 and 7 d, there was no elastin deposition, and minimal collagen deposition was detected (data not shown). After 60 d, both acellular and cellular grafts had extensive collagen deposition in the scaffolds (Fig. 2 *g* and *h*). However, only the MSC-seeded grafts developed an elastic lamina layer adjacent to the lumen (Fig. 2*h*). In the acellular grafts, diffuse elastin staining was found at the border zone between the polymer scaffold and the neointima. These results suggested that ECM structure and components in cellular grafts also mimicked those in native arteries.

Antithrombogenic Property of MSCs *in Vivo*. To elucidate the mechanism of long-term patency and biomimetic remodeling of cellular vascular grafts, we performed short-term experiments to examine the lumen of acellular and cellular grafts. Because thrombosis is the major failure factor of small-diameter vascular grafts, we carried out more detailed analysis on platelet adhesion and thrombus formation. SEM revealed that acellular grafts had significant amounts of platelet aggregation 2 h after implantation, which covered the nanofibrous scaffold (Fig. 3*a*). In contrast, the MSC graft exhibited very little platelet aggregation on the luminal surfaces; MSCs and the underlying nanofibrous scaffold were easily detectable (Fig. 3*b*). Cross-sectional staining also showed thrombus formation on the luminal surface of acellular grafts but not of MSC-seeded grafts (Fig. 3 *c* and *d*). Platelet activation/aggregation and thrombus formation are an immediate host response to foreign-body materials; our results suggested that MSCs could have an antithrombogenic property. Consistently, the results at 60 d showed significant intimal thickening in acellular grafts but not in MSC-seeded grafts (Fig. 3 *e* and *f*). In all experiments, only one acellular graft in a rat was occluded completely. Statistical analysis demonstrated that the lumen area of the cross-sections blocked by intimal tissue was significantly higher in acellular grafts after 1 and 2 months (Fig. 3*g*). Interestingly, intimal thickening stabilized between 1 and 2 months, suggesting that most of the intimal thickening developed within the first month. It is conceivable that the long-term patency of MSC-seeded vascular grafts was mainly because of the antithrombogenic property of MSCs in the early phase.

Antiplatelet Adhesion Property of MSCs *in Vitro*. A dogma in the construction of TEVGs is to use ECs as a cellular layer to prevent thrombosis. To compare the antithrombogenic property of MSCs with that of vascular ECs and SMCs, we performed *in vitro* experiments to determine the platelet adhesion on the surfaces coated with gelatin (positive control), ECs, SMCs, and MSCs. Human platelets were allowed to attach to the surfaces, and CD41 (a platelet-specific marker) was used to identify adherent platelets. As expected, platelets adhered and aggregated on gelatin-coated surfaces (data not shown). MSCs and ECs performed similarly against platelet adhesion (Fig. 4 *a* and *c*), and much more platelet adhesion was observed on the SMC-seeded surfaces (Fig. 4*e*) than those seeded with MSCs or ECs. Quantitative analysis clearly demonstrated significantly lower platelet adhesion/aggregation on MSCs and ECs than that on SMCs (Fig. 4*g*). These results strongly suggest that MSCs can be used as an alternative to ECs for preventing thrombogenesis in vascular reconstruction. To elucidate the underlying mechanism of antiplatelet adhesion/aggregation property of MSCs, we determined the expression of antithrombogenic gene endothelial nitric oxide synthase. However, no endothelial nitric oxide synthase expression was detected in MSCs (data not shown). We postulated that heparan sulfate proteoglycans on the MSC surface might contribute to the MSC resistance to platelet adhesion. To test this possibility, cells were treated with heparinase II to disrupt heparan sulfate proteoglycans. As shown in Fig. 4 *b*, *d*, and *h*, heparinase treatment significantly increased

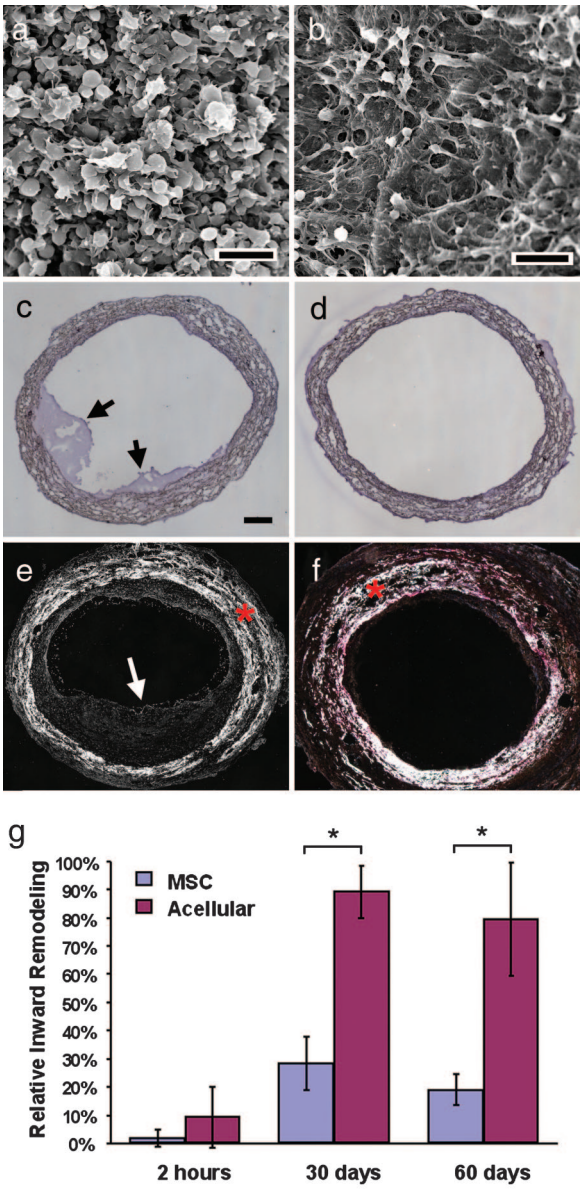

Fig. 3. Antithrombogenic property of MSCs *in vivo*. Images are representatives from at least three independent samples. (*a* and *b*) SEM characterization of the luminal surface of an acellular graft (*a*) and an MSC-seeded graft (*b*) that have been implanted for 2 h. (Scale bar, 5 μm.) (*c* and *d*) H&E staining of cross-sections of an acellular vascular graft (*c*) and a MSC-seeded vascular graft (*d*) that have been implanted for 2 h. Arrows indicate thrombus on the lumen surface. (Scale bar: *c–f*, 100 μm.) (*e* and *f*) Birefringence images of cross-sections of an acellular graft (*e*) and an MSC-seeded graft (*f*) that have been implanted for 60 d. Arrows indicate thrombus/intimal thickening. The white areas marked by red asterisks are PLLA polymers. (*g*) Statistical analysis of intimal inward remodeling in acellular and MSC-seeded grafts. The percentage of the lumen occluded by the intima tissue was quantified by examining birefringence images of cross-sections. *, $P < 0.001$, $n = 3$.

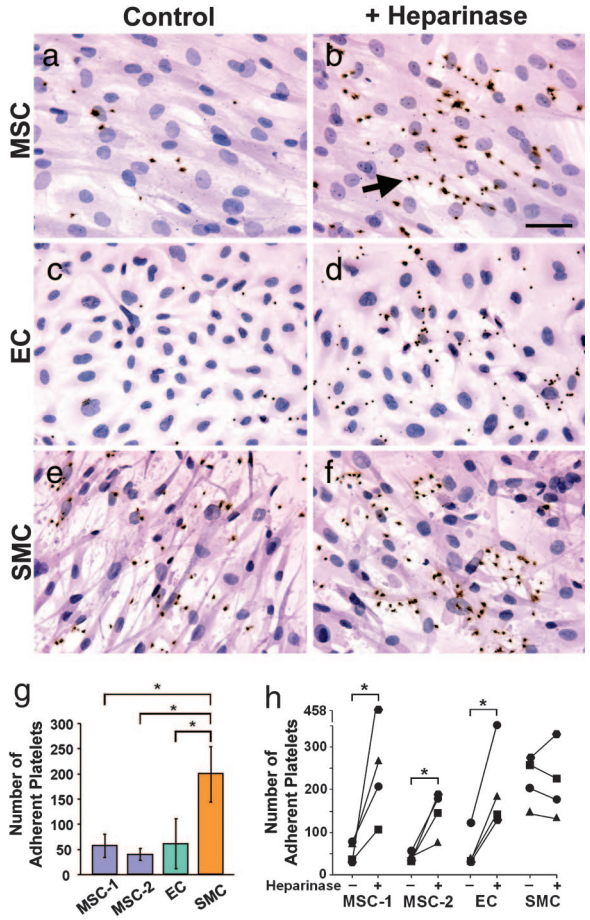

Fig. 4. *In vitro* comparison of ECs, SMCs, and MSCs in platelet adhesion assay. Cells were pretreated with heparinase II (in *b*, *d*, and *f*) or remained untreated (in *a*, *c*, and *e*) before platelet adhesion assay. Human platelets were plated onto culture surfaces seeded with MSCs (*a* and *b*), ECs (*c* and *d*), or SMCs (*e* and *f*). After 30 min, nonadherent platelets were washed away. Platelets were stained by using CD41 antibody (dark brown). (*b*) Arrow indicates an example of platelet staining. MSCs, ECs, and SMCs were visualized by H&E counterstaining. (Scale bar, 20 μm.) (*g*) The number of adherent platelets on MSCs, ECs, and SMCs after 30-min adhesion. The platelets from three donors were used in four experiments. MSC-1 and MSC-2 were from two different donors. *, $P < 0.05$, $n = 4$. (*h*) The effects of heparinase II treatment on platelet adhesion. *, statistically significant difference between the untreated and heparinase-treated samples ($P < 0.05$, $n = 4$).

platelet adhesion/aggregation on MSCs and ECs, suggesting that heparan sulfate proteoglycans play an important role in resisting platelet adhesion/aggregation.

The Fate of MSCs in Vascular Wall. Because both acellular and cellular grafts had efficient EC and SMC recruitment, MSC differentiation might not be a critical factor in the remodeling of cellular grafts in this model. Indeed, staining of the cross-sections of TEVGs after 7 d showed that most of the cells in the wall of TEVGs were from the host [supporting information (SI) Fig. 5], suggesting that the majority of MSCs had short-term engraftment.

Discussion

Our results demonstrate that nanofibrous scaffolds allow the remodeling of vascular grafts in both cellular and ECM content, similar to that of the native artery. The finding of the antithrombogenic property of MSCs has important implication for vascular tissue engineering. The combination of antithrombogenic and nonimmunogenic MSCs with nanofibrous scaffolds is a promising approach to fabricate ideal small-diameter vascular grafts (e.g., autologous or allogeneic) that may be translationally applied to clinical settings.

In this study, we showed that the nanofibrous structure of the scaffolds allowed efficient recruitment of vascular cells and that ECs and SMCs organized into layered structures in the vascular wall, as in the native artery (Fig. 2 *c–f*). Because both acellular

and cellular grafts had extensive recruitment of ECs and SMCs, it is not clear how much MSCs contributed to the cell recruitment process. One interesting observation is the complete endothelialization of both acellular and cellular grafts after 2 months, although significant intimal thickening was present in acellular grafts. Because few MSCs were found in the grafts after 2 months, the ECs should be from the host tissue (e.g., ECs in the surrounding tissue and/or EC precursors from the circulating blood). The relative contribution to endothelialization by the surrounding vascular tissue and the circulating EC precursors awaits further investigation.

Acellular and cellular grafts had similar amount of collagen synthesis (Fig. 2 *g* and *h*). However, the organized structure of elastin was found only in intima/media of cellular grafts. In acellular grafts, there was disorganized and diffused elastin at the interface of the scaffold and the intima. It is possible that intimal thickening resulted in changes of ECM contents (e.g., fibrin vs. collagen) and the functions of the recruited vascular cells, thus interfering with the synthesis and assembly of elastin.

The porous nanofibrous structure, which simulates the native collagen fibril structure, is critical for the remodeling of vascular grafts. The nanofibers could guide and enhance cell migration, and the porous structure allows cell infiltration. The density of the nanofibers is an important parameter. Indeed, when the density of the nanofibers was too high, cell infiltration into the wall of the grafts was inhibited (data not shown). An appropriate nanofiber density is required for efficient cell infiltration while maintaining the mechanical strength of the scaffold. It is interesting that the porous structure of nanofibrous grafts did not have leakage problems upon implantation. It is likely that the multiple layers of nanofibrous structure, the seeded cells, blood cells, and small-scale clotting may all help to prevent the leakage through the graft wall, which needs further investigation.

Another important finding is the antithrombogenic property of MSCs (Figs. 3 and 4). Both *in vivo* and *in vitro* experiments showed the significant suppression of platelet adhesion and aggregation by MSCs. Given that bone marrow MSCs form the niche for hematopoietic cell differentiation and that MSCs are compatible with blood cells in circulation, we argue that MSCs can be a valuable cell source to prevent thrombosis and inflammatory responses. Our data suggest that the antiplatelet adhesion/aggregation property of MSCs depends on cell-surface heparan sulfate proteoglycans, which provides a rational basis for the approach of modifying nanofiber surfaces with antiplatelet adhesion/aggregation molecules.

The short-term engraftment of MSCs (SI Fig. 5) suggests that the long-term patency of cellular grafts could be attributed mainly to the antithrombogenic property of MSCs. Immunohistochemical analysis did not show colocalization of human antigen and vascular cell markers (MHC and CD31) (data not shown), suggesting that MSC differentiation might not be the main contributor of TEVG remodeling. However, besides having an antithrombogenic effect, MSCs could participate in other remodeling processes at the early phase postimplantation, such as ECM remodeling and paracrine signaling, which warrants further studies. The fate of MSCs is not clear. The gradual loss of MSCs may be related to the relative low proliferation rate of MSCs and the removal of MSCs by the host circulation system.

The use of bone marrow stem cells to construct TEVGs should open new avenues for TEVG construction. For example, this approach makes it possible to construct autologous TEVGs by using patients' bone marrow, which provides a solution for patients without suitable autologous grafts and helps to decrease the surgical morbidity and costs associated with the harvest of autologous vessels. Furthermore, a cell bank of MSCs could be easily established and used to fabricate allogeneic vascular grafts at a large scale and could also be available "off the shelf." Alternatively, acellular vascular grafts can be fabricated by modifying the surface of nanofibers to make it antithrombogenic.

Materials and Methods

Cell Culture. Human bone marrow MSCs were obtained from Cambrex (Walkersville, MD). MSCs were cultured in MSC growth medium with prescreened FBS (Cambrex) to allow for cell proliferation without differentiation. MSCs up to passage 10 were used in our experiments. These MSCs were characterized by their surface markers and differentiation potential after cell expansion as described in ref. 18. Human aortic ECs and human aortic SMCs were purchased from Cambrex.

Scaffold Fabrication and Characterization. PLLA (1.09 dl/g inherent viscosity; Lactel Absorbable Polymers, Pelham, AL) was spun to yield randomly oriented nanofibers that were ≈500 nm in diameter, and the fibers were uniaxially aligned by applying 300% strain to the nanofibrous membrane in a 65°C water bath (8). Uniaxial fiber alignment was confirmed by light microscopy, SEM, and the cell morphology on the nanofibers. To determine the mechanical strength of electrospun nanofibrous scaffolds, a sheet of the scaffold (≈0.5 mm thick) was subjected to tensile stretch at 2 cm/min loading rate by using an Instron mechanical test system (Norwood, MA), and Young's modulus was obtained by quantifying the linear part of the stress–strain curve. The PLLA nanofibrous sheets were sterilized in 70% ethanol while under germicidal UV for 30 min before use. The sheet was washed three times in PBS and then immersed in 1% fibronectin (Sigma–Aldrich, St. Louis, MO) for 30 min at 37°C. The sheet was washed once with PBS before cell seeding.

Cell Seeding and Vascular Graft Fabrication. To determine cellular organization on the nanofibrous structure, human SMCs or MSCs were seeded onto aligned nanofibrous membranes in DMEM with 10% FBS and 1% penicillin/streptomycin. After 2 d, the cells were fixed with 4% paraformaldehyde, stained for actin filaments with fluorescein (FITC)-conjugated phalloidin, counterstained by using propidium iodide, and subjected to confocal microscopy (8).

To fabricate cellular vascular grafts, MSCs were seeded on a nanofibrous sheet at a density of ≈100,000 cells per cm^2. The next day, the nanofibrous sheet was wrapped around a 0.7-mm diameter mandrel and bound by a 7-0 suture to maintain the tubular shape. The graft was then removed from the mandrel, resulting in a tubular structure with embedded and circumferentially aligned MSCs. The graft was incubated in culture medium for 2 d before implantation. Acellular grafts were made in the same way except that there was no cell-seeding step.

Live/dead assay (Molecular Probes, Eugene, OR) was used to assess the viability of the MSCs after rolling the nanofibrous sheet. Briefly, the samples were incubated in the culture medium containing 4 μM ethidium bromide (stains dead cells) and 2 μM calcein (stains live cells) for 1.5 h at 37°C, fixed in 4% paraformaldehyde, and immediately visualized by using a Nikon TE300 fluorescence microscope (Melville, NY).

Platelet Adhesion Assay. To compare platelet adhesion on different cell types, human aortic ECs, aortic SMCs, and bone marrow MSCs were seeded in eight-well chamber slides 48 h before blood collection. Blood (15 ml) from healthy human volunteers, free of platelet-active drugs, was drawn from the antecubital vein and immediately anticoagulated with 7:1 vol/vol acid citrate dextrose. After the blood samples were centrifuged at 300 × *g* (10 min) at room temperature, platelet-rich plasma was collected for experiments. Platelet-rich plasma (0.2 ml per well) was gently pipetted onto cells in each well. Platelets on 2.0% gelatin-coated slides were used as a positive control. After incubation for 30 min at 37°C, cells were washed with PBS three times to thoroughly

remove free platelets. After being fixed with 4% paraformaldehyde, cells were blocked with 5% goat serum for 30 min at room temperature and were incubated overnight at 4°C with mouse anti-human CD41 antibody (Lab Vision, Fremont, CA). The samples were incubated with biotin-conjugated secondary antibody and avidin-biotin enzyme reagent (ABC kit; Vector Laboratories, Burlingame, CA) for 1 h. A diaminobenzidine kit was applied to detect adhesive platelets, and a hematoxylin counterstaining was performed. Four areas from each sample were randomly selected, and the numbers of adherent platelets were counted under a microscope with ×40 magnification. The total numbers of adherent platelets from these four images were summed, and the results from multiple experiments from three individual donors were subjected to analysis of variance (ANOVA) to determine the difference in platelet adhesion on MSCs, ECs, and SMCs. A Holm's *t* test was used to determine statistical significance ($P < 0.05$).

To determine the role of cell-surface heparan proteoglycans in preventing platelet adhesion, heparinase II (Sigma–Aldrich) was added at a concentration of 0.22 unit/ml. The cells were washed once with PBS and incubated for 30 min in DMEM with 1% FBS and 1% penicillin/streptomycin in the absence or presence of heparinase II. The cells were washed twice with PBS and used for platelet adhesion experiments. The ratios of the number of adherent platelets between heparinase II-treated and heparinase II-untreated samples were calculated for each donor. A log-transformed *t* test was performed to determine whether heparinase treatment resulted in a statistically significant difference in platelet adhesion for each cell type.

Animal Studies. All procedures were approved by the Institutional Review Board Service and Institutional Animal Care and Use Committee at the University of California, San Francisco. Athymic rats (6–8 weeks old, ≈180 g) were obtained from the National Cancer Institute animal facility. The rats were anesthetized with 2.0% isoflurane and placed in a supine position. A small incision was made to expose and isolate the left CCA. The CCA was clamped and ligated, and the graft was placed end-to-end and sutured with 10-0 interrupted stitches. No heparin or any other anticoagulant was used at any point before or during the implantation procedure. Retrieval of the graft involved the same initial steps for implantation. Forty units of heparin was injected into the external jugular vein to prevent blood clotting during removal of the graft. The graft was removed by ligation of native CCA directly adjacent to the suture locations. For histological analysis, the sample was placed into OCT and cryopreserved at −20°C. Cryosections were taken at 10-μm thickness. For SEM analysis, the samples were preserved in 2% glutaraldehyde, processed, and imaged with a Hitachi S5000 electron microscope (Pleasanton, CA).

Immunohistochemical staining was used to analyze the sections with the following primary antibodies: CD31 (BD Biosciences, San Jose, CA), human-specific nuclear mitotic apparatus protein (NuMA; Santa Cruz Biotechnology), MHC (Santa Cruz Biotechnology, Santa Cruz, CA), and α-actin (Sigma–Aldrich). Collagen and elastin were stained with Verhoeff's Elastic Stain kit (American Master*Tech Scientific, Lodi, CA). Mouse IgG isotype (Dako, Carpinteria, CA) was used in place of primary antibodies for negative controls. Native CCAs from rats served as positive controls for all stains. Immunohistochemistry images were captured with a Zeiss Axioskop 2 MOT microscope (Jena, Germany).

To quantify inward remodeling in the lumen of vascular grafts, cryosections were stained with Verhoeff's elastic stain and imaged with a birefringence filter. The cross-sectional area enclosed by the nanofibrous scaffold and the lumen area (which is decreased by the intimal inward remodeling) was measured with ImageJ Software. The percentage of occluded area in each graft was quantified by using the formula % occluded = $(\text{Area}_{\text{NF}} - \text{Area}_{\text{Lumen}})/\text{Area}_{\text{NF}}$, in which Area_{NF} is the cross-sectional area enclosed by the nanofibrous scaffold in birefringence image. A Student's *t* test was used to determine whether the difference between cellular and acellular group was statistically significant. Two-tailed distribution was used for the analysis.

This work was supported by National Institutes of Health Grants HL 078534 (to S.L.), HL 083900 (to S.L.), P01 NS44155 (to W.L.Y. and G.-Y.Y.), and GM63283-02 (to B.S.H. and B.C.) and California Institute for Regenerative Medicine Training Grant T1-00007 (to C.K.H.).

1. Bognitzki M, Czado W, Frese T, Schaper A, Hellwig M, Steinhart M, Greiner A, Wendorff JH (2001) *Adv Mater* 13:70–72.
2. Li D, Xia Y (2004) *Adv Mater* 16:1151–1170.
3. Huang L, Nagapudi K, Apkarian RP, Chaikof EL (2001) *J Biomater Sci, Polym Ed* 12:979–993.
4. Matthews JA, Wnek GE, Simpson DG, Bowlin GL (2002) *Biomacromolecules* 3:232–238.
5. Yoshimoto H, Shin YM, Terai H, Vacanti JP (2003) *Biomaterials* 24:2077–2082.
6. Kenawy E-R, Layman JM, Watkins JR, Bowlin GL, Matthews JA, Simpson DG, Wnek GE (2003) *Biomaterials* 24:907–913.
7. Xu C, Inai R, Kotaki M, Ramakrishna S (2004) *Tissue Eng* 10:1160–1168.
8. Huang NF, Patel S, Thakar RG, Wu J, Hsiao BS, Chu B, Lee RJ, Li S (2006) *Nano Lett* 6:537–542.
9. Weinberg CB, Bell E (1986) *Science* 231:397–400.
10. Matsuda T, Miwa H (1995) *J Thorac Cardiovasc Surg* 110:988–997.
11. L'Heureux N, Paquet S, Labbe R, Germain L, Auger FA (1998) *FASEB J* 12:47–56.
12. Niklason LE, Gao J, Abbott WM, Hirschi KK, Houser S, Marini R, Langer R (1999) *Science* 284:489–493.
13. Seliktar D, Black RA, Vito RP, Nerem RM (2000) *Ann Biomed Eng* 28:351–362.
14. Caplan AI, Bruder SP (2001) *Trends Mol Med* 7:259–264.
15. Sekiya I, Larson BL, Smith JR, Pochampally R, Cui JG, Prockop DJ (2002) *Stem Cells (Dayton)* 20:530–541.
16. Rasmusson I, Ringden O, Sundberg B, Le Blanc K (2003) *Transplantation* 76:1208–1213.
17. Corcione A, Benvenuto F, Ferretti E, Giunti D, Cappiello V, Cazzanti F, Risso M, Gualandi F, Mancardi GL, Pistoia V, Uccelli A (2006) *Blood* 107:367–372.
18. Wang D, Park JS, Chu JS, Krakowski A, Luo K, Chen DJ, Li S (2004) *J Biol Chem* 279:43725–43734.